

# The stalk connecting the $F_1$ and $F_0$ domains of ATP synthase visualized by electron microscopy of unstained specimens

Edward P. Gogol, Uwe Lücken and Roderick A. Capaldi

*Institute of Molecular Biology, University of Oregon, Eugene, OR 97403, USA*

Received 28 May 1987

*E. coli*  $F_1F_0$  ATP synthase has been reconstituted into membranes and visualized by electron microscopy of unstained samples preserved in thin layers of amorphous ice. Unlike previous observations in negative stain, these specimens are not exposed to potentially denaturing or perturbing conditions, having been rapidly frozen from well-defined conditions in which the enzyme is fully active. The structures visualized in views normal to the lipid bilayer clearly show the presence of a narrow stalk approx. 45 Å long, connecting the  $F_1$  to the membrane-embedded  $F_0$ .

$F_1F_0$ ; ATPase; Cryoelectron microscopy; Energy coupling

## 1. INTRODUCTION

The ATP synthases (ATPases) of energy-converting membranes, including bacterial plasma membranes and chloroplast and inner mitochondrial membranes, are structurally similar in that they consist of two functionally and physically separable parts,  $F_1$  and  $F_0$  (reviews [1,2]). The  $F_1$  portion contains the catalytic sites for ATP synthesis and hydrolysis, and is extrinsic to the membrane. The integral membrane part of the assembly,  $F_0$ , forms the proton channel which couples ATP catalysis to the transmembrane proton gradient.

Electron micrographs of negatively stained specimens of chloroplast and mitochondrial membranes have shown the  $F_1$  part of the ATPase to be separated from the membrane bilayer (and  $F_0$ ) by as much as 50 Å [3,4], leading to the proposal of

a three-domain structure for the assembly, including a stalk between the  $F_1$  and  $F_1F_0$  domains [2]. Selected images of rat liver ATPase, dissolved in the ionic detergent 3-[(3-chloramidopropyl)dimethylammonio]-1-propanesulfate (CHAPS) and stained with uranyl acetate, have been interpreted as tripartite structures consisting of two globular domains joined by a narrow stalk [5]. However, the existence of a stalk between the  $F_1$  and  $F_0$  domains in active ATPase is not universally accepted. The possibility of artifacts generated by the negative staining of specimens for electron microscopy has brought into question the validity of the observations cited above [6–8]. Furthermore, chemical labeling and crosslinking experiments have been interpreted as indicating the close proximity of  $F_1$  and  $F_0$  subunits [9,10], and some models of the ATPase place  $F_1$  and  $F_0$  in direct contact [11].

We are undertaking a structural analysis of the ATPase from *Escherichia coli* ( $ECF_1F_0$ ). This enzyme is the simplest of the ATPases in polypeptide composition, containing only eight subunits:  $\alpha$ ,  $\beta$ ,

Correspondence address: E.P. Gogol, Institute of Molecular Biology, University of Oregon, Eugene, OR 97403, USA

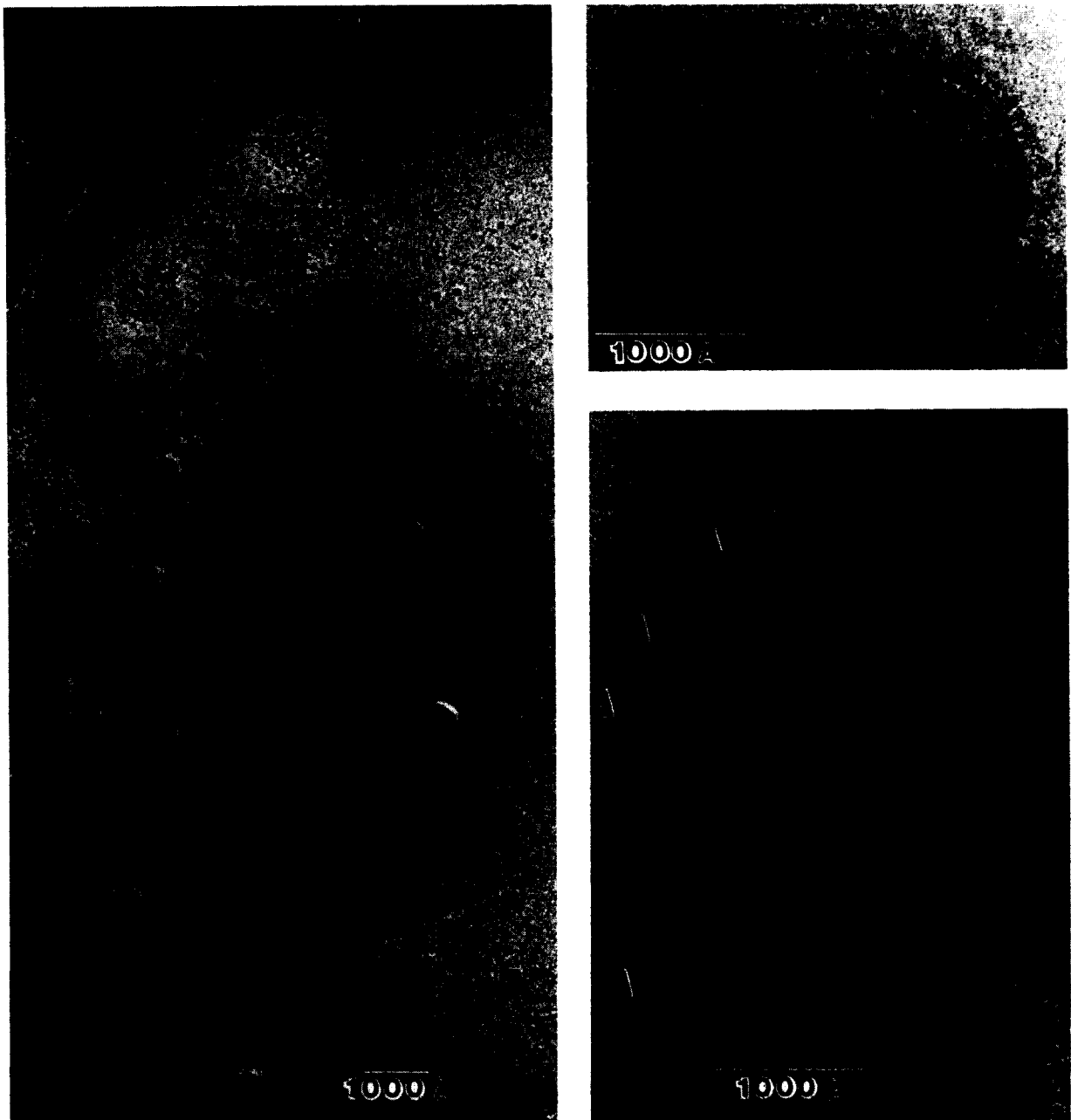


Fig.1. Electron micrographs of unstained  $ECF_1F_0$  complexes, preserved in a thin layer of amorphous ice. (A) An overview of a field of specimens is shown. The holey carbon support film is visible at the left corners of the figure. (B,C) Enlargements of an apparently intact vesicle and a narrow ribbon of membrane, largely in side view, are shown. Note the clearly visible bilayer profile in both micrographs. Arrows point out some of the free  $ECF_1$  molecules visible.

$\gamma$ ,  $\delta$  and  $\epsilon$  in  $F_1$  in 3:3:1:1:1 stoichiometry, and a, b and c in the  $F_0$  in the ratio 1:2:10–12 [1,12]. Here we present electron micrographs of  $ECF_1F_0$  reconstituted into an active, membrane-bound form, which clearly show the presence of a stalk between the  $F_1$  and  $F_0$  domains. The specimens were rapidly frozen from a stable and fully active state, in the absence of stain or other chemical perturbant, and maintained in an amorphously frozen state during microscopy. Analysis of minimal-dose images yields the dimensions of the  $ECF_1F_0$  complex, including those of the stalk.

## 2. MATERIALS AND METHODS

$ECF_1F_0$  was prepared by a modification of the method of Foster and Fillingame [13] from an overproducing strain of *E. coli*, kindly provided by Dr A.E. Senior, University of Rochester. The enzyme was isolated at concentrations of 0.5–1.5 mg/ml protein from sucrose gradients containing 0.4 mg/ml of egg phosphatidylcholine (Sigma), 0.9% sodium cholate (Sigma, recrystallized from ethanol), and 1.5% sodium deoxycholate (Sigma).  $ECF_1F_0$  was reconstituted into membranous form, without the addition of further lipid, by dialysis against buffer [50 mM Tris or 3-(*N*-morpholino)propanesulfonic acid (Mops)] containing 50 mM KCl, 1 mM  $MgCl_2$ , 1 mM dithiothreitol and 20% glycerol, pH 7.5, for 2–3 days at 4°C. These preparations have ATPase activities in the range of 12–20  $\mu$ mol ATP hydrolyzed/min per mg, and exhibit 90–95% inhibition by 20  $\mu$ M *N,N'*-dicyclohexylcarbodiimide (DCCD) reacted for 1 h.

Samples used for electron microscopy were either frozen directly from the above buffer, or dialyzed further to vary the buffer composition, particularly the  $Mg^{2+}$  and glycerol concentrations. Drops of the suspensions (at approx. 1 mg/ml protein) were applied to holey carbon films, blotted to remove excess liquid, and immediately plunged into partially solidified liquid ethane. Specimens were transferred to and stored under liquid nitrogen until insertion into the microscope.

Specimens were loaded into a Gatan cold stage under liquid nitrogen, and examined in Philips EM400 and CM12 electron microscopes, operated at 100 kV. Micrographs were recorded by minimal-dose methods on Kodak S0163 film at

magnifications of 35000–60000. The electron dose varied from approx. 5 to 20  $e^-/\text{\AA}^2$  over this magnification range. Microscope magnifications were calibrated by photographing catalase crystals or calibration grids (Pellico).

Micrographs used for image analysis were chosen from those recorded at  $\times 60000$ , with defocus values sufficiently small to place the first zero of the contrast transfer function outside a resolution of 25  $\text{\AA}$ . Micrographs were digitized using a scanning raster of 25  $\mu$ m, corresponding to 4  $\text{\AA}$  steps at the specimen. Images of individual molecules were selected on the basis of their orientation, clarity, and lack of obvious overlap with their neighbors. The particles were aligned by correlation methods, using the SPIDER image analysis programs [14].

## 3. RESULTS AND DISCUSSION

Electron microscopy revealed the reconstituted  $ECF_1F_0$  preparations to be mixtures of vesicles and sheets of membrane (fig.1A), both covered with  $F_1$  molecules similar to the globular structures visualized in negatively stained preparations [3–5]. The lipid bilayer profiles, approx. 60  $\text{\AA}$  wide, are visible both at vesicle edges and in favorably oriented sheets (fig.1B,C). The sheets were commonly in the form of narrow ribbons of membrane, which were often oriented with the plane of the bilayer approximately normal to the supporting layer of amorphous ice.  $ECF_1$  assemblies extended from both sides of these ribbons (fig.1C), indicating that their orientation in the sheets is scrambled. Specimens were frozen from a variety of buffer conditions, including the presence or absence of 10% glycerol, nucleotides and  $Mg^{2+}$ , without any visible difference in the structures. Very little free  $ECF_1$  was seen if glycerol, nucleotides and  $Mg^{2+}$  were all present, but rather more dissociation of  $F_1$  from the membranes was noted if some or all of these reagents were omitted.

For an initial analysis of the  $ECF_1F_0$  images, 40 molecules were selected from three different micrographs. The chosen particles were incorporated in sheets which appeared to be oriented along the beam direction, as judged by the thickness of the bilayer and visibility of its distinctive three-layered profile. Similar images were visible at vesicle edges, but were not chosen for

analysis because of the difficulty of assessing their orientation and the problems inherent in the curvature of the membrane. Ten of the images were discarded due to the obviously poor alignment of the major features (the  $F_1$  domain and the lipid bilayer). The remaining particles were averaged to yield the side view of the  $ECF_1F_0$  shown in fig.2A. The aligned particles were also visually subdivided into classes based on the appearance of the  $ECF_1$  portion. Ten images from each of two obvious categories, those with a bilobed  $F_1$  and those with a more solid  $F_1$  domain, were selected to make up the averages shown in fig.2B and C.

All of the averaged  $ECF_1F_0$  images shown in fig.2 have consistent overall dimensions: a membrane thickness of 60 Å,  $ECF_1$  dimensions of approx. 110 by 90 Å normal and parallel to the bilayer, respectively, and a separation from the bilayer of approx. 45 Å. The  $ECF_1$  is linked to the  $ECF_0$  by a narrow stalk, often visible in individual images, and clearly visible in the averages. The thickness of the stalk appears to be about 20 Å, though this measurement is at the limit of the resolution of these micrographs. Two classes of

views of the  $ECF_1$  are represented most often in the filtered images: those with a relatively solid appearance and those with an apparent cleft normal to the membrane. Few of the particles examined have the pseudohexagonal structure commonly seen both in negatively stained  $F_1$  [15–18] and unstained free  $ECF_1$  (arrows, fig.1C). The different images of membrane-bound  $ECF_1$  are probably different projections of otherwise identical molecules, rotated about an axis parallel to the stalk. However, different states of the enzyme may also be represented. We hope to understand further the spatial relationship of  $ECF_1$  to  $ECF_0$  by analysis of a more extensive set of views of both  $ECF_1F_0$  and free  $ECF_1$ .

The most important result of this preliminary analysis is the clear evidence for the presence of a stalk joining the  $ECF_1$  and  $ECF_0$  domains. It has been visualized by electron microscopy of  $ECF_1F_0$  in the absence of negative stain or other chemical or mechanical perturbant. This structure is close to 50 Å long and only about 20 Å wide, approximately the size of four to five closely packed  $\alpha$ -helices. It must serve to couple proton translocation across

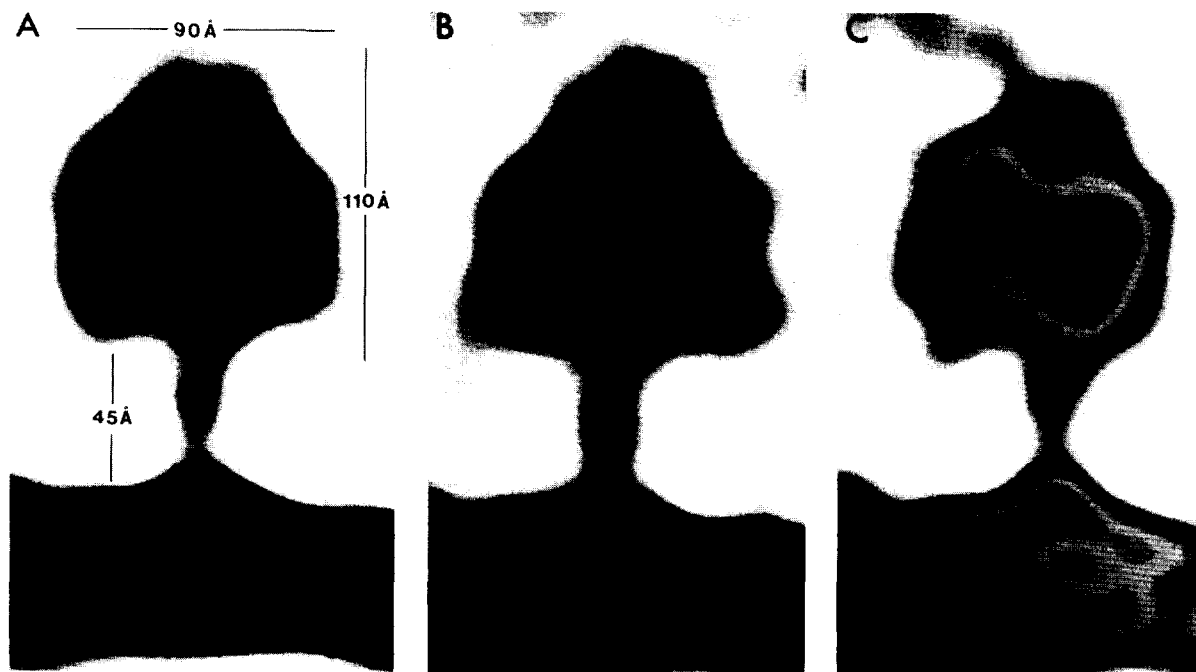


Fig.2. Averages of side views of  $ECF_1F_0$  were computed from (A) all 30 particles which aligned well by correlation methods; (B) 10 particles which have a cleft in the  $ECF_1$  domain; (C) 10 particles with a more solid  $ECF_1$  domain.

the membrane (via the ECF<sub>0</sub>) to the synthesis or hydrolysis of ATP by the ECF<sub>1</sub>. Coupling could be by proton transfer along a channel through the ECF<sub>0</sub> and the stalk, a distance in excess of 100 Å. It is unlikely that vectorial proton movement can be insulated from the surrounding aqueous phase in a structure as narrow as the stalk. A more probable coupling mechanism is a conformational change in the stalk, induced by proton transfer across the membrane, which is then transmitted to the catalytic sites in the ECF<sub>1</sub>. A similar long-range conformational change is required to explain the inhibitory effect of DCCD modification of subunit c of ECF<sub>0</sub> on the binding of nucleotides in the catalytic sites of ECF<sub>1</sub> [19].

#### ACKNOWLEDGEMENTS

We thank Dr Nigel Unwin for use of his facilities for some of the electron microscopy and image analysis, and Dr Robert Aggeler and Ms Patricia Ryan for isolation of the ECF<sub>1</sub>F<sub>0</sub>. This work was supported by NIH grant HL24526 to R.A.C., and NATO training fellowship 300-402-503-6 from the DAAD to U.L.

#### REFERENCES

- [1] Senior, A.E. and Wise, J.G. (1983) *J. Membrane Biol.* 73, 105–124.
- [2] Amzel, L.M. and Pederson, P.L. (1983) *Annu. Rev. Biochem.* 52, 801–824.
- [3] Fernandez-Moran, H., Oda, T., Blair, P.V. and Green, D.E. (1964) *J. Cell Biol.* 22, 63–100.
- [4] Telford, J.N., Langworthy, T.A. and Racker, E. (1984) *J. Bioenerg. Biomembranes* 16, 335–351.
- [5] Soper, J.W., Decker, G.L. and Pederson, P.L. (1979) *J. Biol. Chem.* 254, 11170–11176.
- [6] Sjöstrand, F.S., Andersson-Cedergren, E. and Karlsson, U. (1964) *Nature* 202, 1075–1078.
- [7] Malhotra, S.K. and Eakin, R.T. (1967) *J. Cell Sci.* 2, 205–212.
- [8] Wainio, W.W. (1985) *J. Ultrastruct. Res.* 93, 138–143.
- [9] Hackney, D.D. (1980) *Biochem. Biophys. Res. Commun.* 94, 875–880.
- [10] Aris, J.P. and Simoni, R.D. (1983) *J. Biol. Chem.* 258, 14599–14609.
- [11] Bragg, P.D. and Hou, C. (1980) *Eur. J. Biochem.* 105, 495–503.
- [12] Walker, J.E., Saraste, M. and Gay, N. (1984) *Biochim. Biophys. Acta* 768, 164–206.
- [13] Foster, D.L. and Fillingame, R.H. (1979) *J. Biol. Chem.* 254, 8230–8236.
- [14] Frank, J., Shimkin, B. and Dowse, H. (1981) *Ultramicroscopy* 6, 343–358.
- [15] Akey, C.W., Crepeau, R.H., Dunn, S.D., McCarty, R.E. and Edelman, S.J. (1983) *EMBO J.* 2, 1409–1415.
- [16] Tiedge, H., Schäfer, G. and Mayer, F. (1983) *Eur. J. Biochem.* 132, 37–45.
- [17] Boekema, E.J., Berden, J.A. and Van Heel, M.G. (1986) *Biochim. Biophys. Acta* 851, 353–360.
- [18] Lücken, U., Bork, T., Remington, S.J. and Capaldi, R.A. (1987) *Biochim. Biophys. Acta*, submitted.
- [19] Penefsky, H.S. (1985) *Proc. Natl. Acad. Sci. USA* 82, 1589–1593.